Coverage and Effective Capacity in Downlink MIMO Multicell Networks with Power Control: Stochastic Geometry Modelling

Murtadha Al-Saedy, H. S. Al-Raweshidy, *Senior Member, IEEE,* Hussien Al-Hmood, *Member, IEEE,* and Fourat Haider

M. Al-Saedy, H. S. Al-Raweshidy, and Hussien Al-Hmood (corresponding author) are with wireless network communications centre (WNCC), College of Engineering, Design and Physical Sciences, Brunel University London, Uxbridge, UB8 3PH, U.K. (e-mail: {Murtadha.Al-Saedy, hamed.al-raweshidy, Hussien.Al-Hmood}@brunel.ac.uk).

F. Haider (corresponding author) is with Hutchison 3G UK, 20 Grenfell Rd., Maidenhead, SL6 1EH, U.K. (e-mail: Fourat.haider@three.co.uk).

Abstract

In this paper, coverage probability and effective capacity in downlink multiple-antenna cellular system are considered. Two scenarios are investigated; in the first scenario, it is assumed that the system employs distance-based fractional power control with no multicell coordination. For the second scenario, we assume the system implements multicell coordinated beamforming so as to cancel inter-cell interference. For both scenarios, the BSs are assumed to randomly uniformly distributed in the area according to Poisson point process (PPP). Using tools from stochastic geometry, tractable, analytical expressions for coverage probability and effective capacity are derived for both scenarios. Numerical results reveal that for a system with stringent delay QoS constraints, i.e. (traffic delay is intolerable), best performance can be achieved by suitably adopting fractional power strategy when transmitting to the users, while constant power allocation performs better than all other power allocation strategies when the delay QoS constraints get loose (tolerable delay). For coverage probability, a fractional power control is better than constant power and channel inversion power strategies for low signal-to-interference plus noise ratio (SINR) thresholds, while the constant power strategy performs better than others in high SINR thresholds.

Index Terms

Coverage probability, Effective capacity, stochastic geometry, fractional power control, multiple-input multiple-output (MIMO), coordinated MIMO, beamforming.

I. INTRODUCTION

With the rapidly growing number of smart phones and the ever-increasing demands for services such as web browsing, multimedia services, and video streaming, future wireless networks are expected to support high data rate services with diverse quality of service (QoS) requirements [1]- [3]. The delay-sensitive applications impose the challenge of the service reliability, where different delay QoS requirements are to be guaranteed to the end users [2]. As a response to these challenges, a great part of research has been devoted to develop highly spectrally efficient wireless network technologies [4], [5]. Consequently, wireless networks nowadays tend to be more densified with aggressive frequency reuse [4]. However, this comes at the price of higher inter-cell interference experienced by users at the cell-edge, resulting in degradation in system performance of the currently deployed mobile systems [4].

The framework adopted for evaluating cellular systems is mainly based on the concept of Shannon capacity [6]. Shannon capacity dictates the maximum achievable data rate achievable in the system, and is related to coverage, which is the distribution of signal-to-noise and interference ratio (SINR) in the cellular system. While this information-theoretic framework is suitable for an analysis of system spectral efficiency, it does not impose any delay QoS constraints [7]. Thus, for future wireless network with diverse delay QoS requirements, it is necessary to account for delay QoS constraints when analysing the whole system performance [7]- [9] so as to evaluate the the system capability of QoS provisioning. To this end, a powerful concept termed as effective capacity is proposed in [10], it gives maximum arrival rate that a given service process can support so that a QoS requirement specified by a certain QoS measure can be guaranteed [10]. Hence, it gives the statistical QoS guarantees [7], where delay is required to be lower than a threshold value only for a certain percentage of time. The effective capacity is known to be the dual of effective bandwidth previously studied in wired networks [11], [12]. Using this effective capacity concept, the delay-QoS constraint is characterized by the QoS exponent θ such that a small value of θ corresponds to a looser QoS constraint (no delay constraint), i.e. (system can tolerate an arbitrarily long delay), and the effective capacity is reduced to Shannon capacity. While a larger value of θ corresponds to the case of stringent delay QoS constraint [13]. Based on the effective capacity concept, various scheduling and power allocation schemes are proposed for single cell scenario. In [13], [14], the optimal rate and power adaptation policies are analysed for effective

capacity maximization. In [7], the tradeoff between power and delay is characterised assuming only noise with no interference. In [10], [15], TDMA-based scheduling scheme for cellular networks is developed. In [17], [15], it is shown that when the QoS constraint gets looser, the optimal power allocation converges to the classical water-filling that achieves Shannon capacity, while it converges to the scheme operating at a constant rate, i.e., channel inversion. For efficient QoS provisioning, the two main wireless resources, i.e. power and bandwidth, should be very efficiently utilised, and algorithms for this purpose are introduced in [16], [17]. In this regard, power control has also been utilised to guarantee that SINR is above a target value required to maintain wireless communication, hence resulting in better QoS. All the aforementioned works are only limited to single cell scenario, hence, they do not consider a cellular systems with inter-cell interference, where the inter-cell interference has non-negligible impact. To the best of authors knowledge, no work has yet been done for analysing effective capacity in multicell scenario. To bridge the gap in this area and characterise delay QoS using effective capacity in interference-limited cellular networks, analytical framework is necessary from this perspective.

The traditional deterministic multicell models, namely hexagonal, lattice, and Wyner models, have been extensively utilised for evaluating cellular networks performance [18]. However, in reality, BSs are generally non-regularly-deployed; therefore the deterministic hexagonal models are not sufficient for predicting the real system performance. Moreover, hexagonal and lattice deterministic models do not allow tractability in the analysis [18]. The inadequacy of the aforementioned models has motivated the research towards using random spatial models for analysing cellular systems [18], [19]. The advantage of random spatial models is that they allow analytical tractability and lead to closed-form or semi closed-form expressions for the main system performance metrics, such as capacity, coverage probability. Furthermore, they are more accurate for analysing densely-deployed networks that are rapidly gaining interest nowadays [18].

Power control is an important technique that has been widely studied in multicell networks. Power control to compensate the effect of small-scale fading is studied in [20], however, such power allocation strategy requires the knowledge of instantaneous channel state information (CSI) at each scheduling instant, hence imposing heavy feedback signalling. Moreover, the signal attenuation due to path-loss may outweigh the signal deterioration caused by small-scale fading. Thus, small-scale fading based power control may not always be the suitable strategy for QoS provisioning, and therefore it is worth considering distance-based power control that keeps the

average SINR at a certain level necessary to signal decoding. Distance-dependent power control is proposed for downlink systems in [21], [22], and uplink systems in [23]. In [22], discrete power allocation scheme is proposed for ad hoc systems.

Unlike the aforementioned works, we consider multiple-input-multiple-output (MIMO) downlink random cellular system employing fine-grained (continuous) distance-based fractional power control, and analyse coverage probability and effective capacity for this system. The locations of BSs are modelled as point Poisson process (PPP) [18], [19], whereby stochastic geometry provides mathematical tools for dealing with such random processes. We consider two scenarios of cellular networks. In the first scenario, it is assumed that distance-based power control is employed by each BS when transmitting to its respective users, and it is assumed that no coordination among BSs to cancel the interference takes place. Under this scenario, two cases are investigated; single user MIMO (SU-MIMO) and multiuser MIMO (MU-MIMO). In SU-MIMO, a BS serves only one user over single frequency-time slot via maximum ratio transmission (MRT) technique. For MU-MIMO, on the other hand, the system utilises zero forcing (ZF) technique to spatially multiplexes several multiple users data for simultaneous transmission, this technique is known under the name of space division multiple access (SDMA).

In the second scenario, we further assume that several BSs can form a cluster and coordinate their transmission so as to cancel the inter-cell interference at the unintended users by using coordinated beamforming (CB) technique. Although, cancelling out interference is beneficial in general, however, it comes at the price of loosing degrees of freedom. Therefore, we conduct our analysis based on coordination range (the relative distance between the serving and last BS involved in coordination). The coordination range can generally determine whether it is more useful to coordinate or it might be better to transmit using the maximum eigen mode of transmission channel. For both scenarios, we derive analytical expressions for coverage probability, which is an important performance metric in the classical information-theoretic approach. To characterise the delay QoS, analytical expression for effective capacity is derived based on coverage probability analysis. Henceforth, coverage probability analysis is introduced first, and, subsequently, effective capacity is derived.

The main contributions of the paper are as follows

- We study and analyse coverage probability and effective capacity for MIMO cellular systems employing distance-based fractional power control and no multicell coordination is assumed.

Two cases have been considered and analysed; SU-MIMO and MU-MIMO. Analytical expressions are derived for coverage probability, subsequently the effective capacity is derived in terms of coverage probability. Moreover, closed-form expressions are derived for Laplace term accounting for interference for spacial cases power control factors.

- We study and analyse the coverage probability of MIMO cellular systems employing interference cancellation using multicell MIMO coordination. The coverage probability is defined as a function of coordination range inside which the coordination takes place. Analytical expression is derived for coverage probability of such scenario.

- We model the locations of BSs as random PPP model for both scenarios, where we use tools from stochastic geometry to analyse coverage probability and effective capacity.

Organization: Section II describes the system model of the analysed cellular system. Section III presents the main results of coverage analysis for SU-MIMO and MU-MIMO with power control and no interference cancellation. In Section IV, the analytical result of coverage probability with interference cancellation is presented. In Section V, analytical expression for effective capacity is introduced. Section VI presents simulation and numerical results. Finally, conclusions are drawn in Section VII.

Notations: Bold and lowercase letters denote vectors. The notations $(.)^{\mathsf{H}}$ and $\| \, . \, \|$ denote conjugate transpose and norm of a vector, respectively. $\mathbb{E}\{.\}$ is the expectation operator, while $\mathbb{E}_x\{.\}$ denotes the expectation with respect to x. $\Gamma(k)$ stands for gamma function defined as: $\int_0^\infty x^{k-1}e^{-x}\mathrm{d}x$. $\mathbb{P}[a > b]$ is the probability that the inequality $\mathrm{a} > \mathrm{b}$ holds true. $P_{|x}[y]$ is the conditional probability of y given that x has already been given.

II. System Model

We consider a downlink multicell cellular system. BSs, each equipped with N_t antennas, are positioned in a two-dimensional horizontal plane as a homogeneous spatial PPP Φ with density λ. In PPP, the number of nodes, e.g. BSs in a given bounded area A is a random variable (r.v.) following Poisson distribution with their positions being uniformly distributed. When the association policy for users is to connect to the nearest BS, the cell boundaries are shown to be Voronoi tessellation [18], as shown in Fig. 1. Since we consider a homogeneous PPP, the statistics evaluated for every node in the system will be similar. Hence, we will perform our analysis based on a typical user at the origin. This is justified by Slivnyak's [18], [19], which

states that the statistical properties observed by a typical point of the Φ are similar to those observed by a point at the origin in the process $\Phi \cup \{0\}$. The BSs distances from this typical user are given according to the homogeneous PPP, $\Phi = \{r_k, k \in \mathbb{N}\}$, on the two dimensional plane $\mathbb{R}^2$, where r_k denotes the distance from the kth BS. The user is assumed to be associated with the nearest base station denoted as BS_1 and located at distance r_1 from it. While all other BSs ($\mathrm{BS}_k, k \in \Phi$) are regarded as interferers to this user as shown in Fig. 1. Notice that the distance between a typical user and the kth BS is a r.v. following generalised Gamma distribution given by [26]

$$f_{r_k}(r) = \frac{2(\lambda \pi r^2)^k}{r \Gamma(k)} e^{-\lambda \pi r^2} \tag{1}$$

We assume that each user is equipped with a single-antenna.

Assuming that each user is able to estimate its downlink channel perfectly and feed CSI back to its serving BS by means of dedicated pilot signal. If the user is assumed to be helped through coordination it should also estimate its channels to $K - 1$ BSs and feed them back to its serving BS, whereby they are conveyed to the other BSs through delay-free unlimited capacity links.

Let us denote the downlink small-scale channel vector between the typical user and kth BS as $\mathbf{h}_k = [h_1, ..., h_{N_t}] \in \mathbb{C}^{1 \times N_t}$, where each component of $\mathbf{h}_k$ are an independent and identically distributed (i.i.d) complex Gaussian r.v with zero mean and unit variance, i.e. $\mathcal{CN}(0, 1)$. In this paper, we consider two beamforming techniques, MRT and ZF, which are defined as follows

1- *MRT Beamforming*: MRT beamforming vector is constructed such that it is aligned to the channel direction, i.e. if the channel vector is $\mathbf{h}$, the beamfomer is constructed as [24].

$$\mathbf{v} = \frac{\mathbf{h}^\mathsf{H}}{\| \mathbf{h} \|} \tag{2}$$

2- *ZF*: for MU-MIMO, let $\mathbf{H} = [\mathbf{h}_1 \mathbf{h}_2 ... \mathbf{h}_K]$ denote the aggregate channel matrix of K users. The ZF beamforming vectors $\mathbf{v}_1, ..., \mathbf{v}_K$ can be chosen to be the normalised columns of the matrix [24]

$$\mathbf{V} = \mathbf{H}^\dagger = \mathbf{H}^\mathsf{H}(\mathbf{H}\mathbf{H}^\mathsf{H})^{-1} \tag{3}$$

For interference cancellation via CB, a BS with N_t can cancel interference for up to $K = N_t - 1$ users using ZF technique. As an example for a given nth user with channel vector $\mathbf{h}_n$, the beamforming precoder vector can be obtained by projecting the vector $\mathbf{h}_n$ on the

null space of $\hat{\mathbf{h}}_n = \left[\mathbf{h}_1^{\mathsf{H}}, ..., \mathbf{h}_{n-1}^{\mathsf{H}}, \mathbf{h}_{n+1}^{\mathsf{H}}, ..., \mathbf{h}_K^{\mathsf{H}}\right]^{\mathsf{H}}$ [24]

$$\mathbf{v}_n = (\mathrm{I} - \mathcal{P}_{\hat{\mathbf{h}}_n})\mathbf{h}_n \tag{4}$$

where $\mathcal{P}_{\hat{\mathbf{h}}_n}$ denotes the projection on $\hat{\mathbf{h}}_n$, given as $\mathcal{P}_{\hat{\mathbf{h}}_n} = \hat{\mathbf{h}}_n^{\mathsf{H}}(\hat{\mathbf{h}}_n\hat{\mathbf{h}}_n^{\mathsf{H}})^{-1}\hat{\mathbf{h}}_n$.

The channel distribution of MIMO link is quite different from single antenna link. For single antenna links, the channel is exponentially distributed for both direct and interfering links. While for the link from multi-antenna BS to a single-antenna user the channel distribution depends on the MIMO transmission technique and whether a BS is serving or interfering. This is because when transmitting to a user, the BS precodes its signal for its intended user, hence resulting in different effective channel distribution from the case when it acts as an interferer.

The effective channel of both direct and interfering links denoted as g_0 and g_i, respectively, where $g_n = |\mathbf{v}_n^{\mathsf{H}}\mathbf{h}_k|^2$, is an i.i.d r.v. following gamma distribution, i.e. $\Gamma(\Delta, 1)$ and $\Gamma(\Psi, 1)$, respectively [25]. Δ and Ψ are the shape parameters of gamma distribution.

Now, we describe the main two scenarios studied in this work as follows

- *Fractional power control and no coordination*: in this scenario, we assume that the system does not implement multicell coordination, while employing distance-based fractional power control. Two cases are studied under this scenario; SU-MIMO and MU-MIMO. Each BS makes use of power control to compensate for path-loss attenuation experienced by its served user. More specifically, each ith BS allocates power proportional to the user distance, $X_i^{\alpha\eta}$, where $\eta \in [0, 1]$ is the fractional power control factor, and X_i represents the distance from ith interfering BS to its served user. Likewise, for MU-MIMO each user is allocated power proportional to its distance from the BS. Since $X_1 = r_1$ the desired signal power at the typical user becomes $g_0 r_1^{\alpha(\eta-1)}$. Moreover, the interference power from each interfering BS becomes $(X_i^{\alpha})^{\eta} g_i r_i^{-\alpha}$. Thus, a user closer to its serving BS demands less power than required by a user farther away. Under this system model, the signal-to-noise and interference ratio ($SINR$) can be written as

$$SINR = \frac{g_0 r_1^{\alpha(\eta-1)}}{\sigma^2 + I} \tag{5}$$

where $I = \sum_{i \in \Phi/\{\mathrm{BS}_1\}} X_i^{\alpha\eta} g_i r_i^{-\alpha}$ is the aggregate interference experienced at the typical user, and σ^2 represents the additive noise power which is assumed to be constant. Note that for SU-MIMO using MRT, $\Delta = N_t$ and $\Psi = 1$, while for MU-MIMO utilising ZF,

we have $\Delta = N_t - \Psi + 1$, where Ψ is the number of users served by MU-MIMO. It is worth noting that for single antenna links, $\Delta = \Psi = 1$, which is equivalent to exponential distribution, the interested reader can refer to [25] for more details.

- *Multicell coordination*: in this scenario, we assume that a cluster of BSs are able to coordinate their beamforming to eliminate inter-cell interference at each unintended user. For simplicity in analysis, let use assume SU-MIMO and $\eta = 0$, however the analysis can be straightforwardly generalised to MU-MIMO and any power control strategy. Thus, $SINR$ for such scenario becomes

$$SINR = \frac{g_0 P r_1^{-\alpha}}{\sigma^2 + I_c} \tag{6}$$

where P is the transmit power, and

$$I_c = \sum_{i \in \Phi/\{\mathrm{BS}_1,...,\mathrm{BS}_K\}} g_i P r_i^{-\alpha} \tag{7}$$

is the aggregate inter-cell interference from all BSs except the set of BSs $\{\mathrm{BS}_1, ..., \mathrm{BS}_K\}$. Recall that $g_0 \sim \Gamma(\Delta, 1)$ and $g_i \sim \Gamma(\Psi, 1)$, with $\Delta = N_t - K + 1$ and $\Psi = 1$ [25].

A. Effective Capacity

Now, we briefly introduce the concept of effective capacity concept (E_c). Consider a queuing system of a typical BS with constant arrival rate as shown in Fig. 1. The arriving packets are stacked in the buffer for transmission in time slot T_s, over a subband of bandwidth denoted as W. The statistical delay QoS for this system can be defined as the probability for the queue length of the transmitter buffer exceeding a certain threshold x decays exponentially as a function of x, therefore the QoS exponent θ can be defined as [13]- [14]:

$$\theta = -\lim_{x \to \infty} \frac{\ln\big(\mathbb{P}\big[\mathrm{q}(\infty) > x\big]\big)}{x} \tag{8}$$

where $\mathrm{q}(\mathrm{t})$ denotes the buffer length at time t. Notice that $\theta \to 0$ implies no delay constraint required in the system, whereas $\theta \to \infty$ corresponds to system with a strict delay constraint, therefore θ is considered as the delay QoS constraint of the system [10]. Accordingly, the E_c is defined as [10]:

$$E_c = \frac{\Lambda(-\theta)}{-\theta} = -\lim_{n \to \infty} \frac{1}{n\theta} \ln\left(\mathbb{E}\left\{e^{-\theta \sum_{i=1}^{n} R[i]}\right\}\right) \tag{9}$$

where $R[i]$ is the transmission rate in time slot i defined as:

$$R[i] = T_s W \ln\left(1 + SINR\right) \tag{10}$$

Hereafter, we assume $T_s W = 1$ [13]. Assuming that the stochastic service process is independent and identically distributed (i.i.d) process, i.e. stationary and ergodic process, E_c in (9) can be simplified to [13]- [16]

$$E_c = -\frac{1}{\theta}\ln\left(\mathbb{E}\{e^{-\theta R[n]}\}\right) = -\frac{1}{\theta}\ln\left(\mathbb{E}\left\{1 + SINR\right\}^{-\theta}\right) \tag{11}$$

Thus, QoS can be incorporated in the scheduling process of the system by interpreting θ exponent as the QoS requirement. Thereby, the effective capacity is maximised for a given θ instead of the conventional approach in which the throughput is maximised subject to delay constraint.

III. COVERAGE PROBABILITY ANALYSIS: NO INTERFERENCE CANCELLATION

In this section, analytical expressions are derived for coverage probability for a typical user in MIMO system. We first introduce the coverage of SU-MIMO with power control, then we proceed to analyse the coverage of MU-MIMO. The coverage probability, i.e., the probability of achieving the target $SINR$ $\bar{\gamma}$ at the typical user can be defined as $\mathbb{P}[SINR > \bar{\gamma}]$, which is equivalent to the complementary cumulative distribution function CCDF of the $SINR$ [19]. Coverage probability can also be interpreted as the average fraction of the network area (users) for which (for whom) $SINR$ is greater than $\bar{\gamma}$.

A. Coverage Probability with SU-MIMO

Now we focus on the coverage probability of SU-MIMO with power control. An upper bound for coverage is introduced in the following theorem.

Theorem 1: The upper bound on the coverage probability for SU-MIMO system employing distance-based fractional power control, P_c^{SU}, is given by:

$$P_c^{\mathsf{SU}} \leq \sum_{m=1}^{N_t} \binom{N_t}{m}(-1)^{m+1} \int_0^\infty 2\pi\lambda r_1 e^{-(\pi\lambda r_1^2 + \bar{\gamma}m\zeta r_1^{\alpha(1-\eta)}\sigma^2)}\exp(-2\pi\lambda\psi)\mathrm{d}r_1 \tag{12}$$

where

$$\psi = \mathbb{E}_X\left\{\frac{\bar{\gamma}m\zeta r_1^{(2-\alpha\eta)}X^{\alpha\eta}}{\alpha-2}{}_2F_1\left(1, 1-\frac{2}{\alpha}; 2-\frac{2}{\alpha}; -\bar{\gamma}m\zeta r_1^{-\alpha\eta}X^{\alpha\eta}\right)\right\}, \tag{13}$$

$\zeta = (N_t!)^{\frac{-1}{N_t}}$, and

$$_pF_q(a_1, .., a_p; b_1, ...b_q; z) = \sum_{n=0}^{\infty} \frac{(a_1)_n...(a_p)_n}{(b_1)_n...(b_q)_n} \frac{z^n}{n!} \qquad (14)$$

is the hypergeometric function, where $(a)_n$ denotes the Pochhammer symbol representing the falling factorial [27].

Proof: See Appendix A.   ■

The lower bound for the coverage probability can be obtained by setting $\kappa = 1$. Furthermore, it can be observed that the bound is closed for single-input single-output (SISO), i.e. $N_t = 1$. The expressions in the above results involve double integrations, however the expectation in (13) can be further simplified using the following corollary.

Corollary 1: For the (13), closed form expressions can be obtained for special cases defined below: When $\alpha = 4, \eta = 0$, ψ is given by:

$$\psi = \frac{r_1^2 \bar{\gamma} m \zeta}{\alpha - 2} {}_2F_1 \left(1, 0.5; 1.5; -\frac{\bar{\gamma} m \zeta r_1^2}{\pi \lambda} \right) \qquad (15)$$

Proof: See the Appendix B.   ■

Note that this case corresponds to constant power allocation. Following the same steps in Appendix B, (13) can be also obtained in closed form for other two special cases. When $\alpha = 4, \eta = 1$, ψ is given by:

$$\psi = \frac{2\bar{\gamma} m \zeta}{(\lambda \pi r_1)^2 (\alpha - 2)} {}_4F_1 \left(1, 0.5, 1.5, 2; 1.5; -\frac{4\bar{\gamma} m \zeta}{(\pi \lambda)^2 r_1^4} \right) \qquad (16)$$

This case corresponds to full-channel inversion. When $\alpha = 4, \eta = 0.5$, ψ is given by:

$$\psi = \frac{\bar{\gamma} m \zeta}{\lambda \pi (\alpha - 2)} {}_3F_1 \left(1, 0.5, 2; 1.5; -\frac{\bar{\gamma} m \zeta}{\pi \lambda r_1^2} \right) \qquad (17)$$

This case corresponds to the fractional power control. For the other values of α and η, the integration should be evaluated numerically.

B. Coverage Probability with MU-MIMO

When the system utilises SDMA to serve multiple users, a number of Ψ users can be served simultaneously over the same frequency band and time slot. Since the users have different positions from the BS, each user will be allocated an amount of power based on its distance from its serving BS. This, however, may lead to more analysis complexity. For tractability of analysis, let us assume that the set of scheduled users served via SDMA are located on equal distances from their serving BS, hence, they will be allocated the same amount of power. Alternatively, we

can also assume that the users are located at different distances from the serving BS, however, they will be allocated an equal amount of power proportional to farthest user distance from its serving BS. These assumptions significantly render the analysis more tractable.

In the following theorem, an exact analytical expression of coverage probability for MU-MIMO is presented.

Theorem 2: The coverage probability of a typical user served via full-SDMA in MU-MIMO employing distance-based fractional power control is given by

$$P_c^{\mathsf{MU}} = \int_0^\infty 2\pi\lambda r_1 e^{-(\pi\lambda r_1^2 + \bar{\gamma} r_1^{\alpha(1-\eta)}\sigma^2)}\exp(-2\pi\lambda\psi)\mathrm{d}r_1 \tag{18}$$

where

$$\psi = \mathbb{E}_X\left\{\sum_{m=1}^{\Psi}\binom{\Psi}{m}\frac{r_1^{2-m\alpha\eta}X^{m\alpha\eta}\bar{\gamma}}{m\alpha-2}{}_2F_1\left(\Psi, m-\frac{2}{\alpha}; m+1-\frac{2}{\alpha}; -\frac{\bar{\gamma}r_1^{\alpha(1-\eta)}X^{\alpha\eta}}{r_1^\alpha}\right)\right\} \tag{19}$$

Proof: See the Appendix C. ∎

It is worth noting that the expectation in (19) can be obtained in closed form in special cases as in Corollary 1. Note that the above result is tight for full-SDMA, i.e. the number of users served by each BS is equal to the number of transmit antennas ($\Delta = N_t - \Psi + 1$). Otherwise, an upper bound should be sought for coverage probability in a similar manner to SU-MIMO analysis.

IV. COVERAGE PROBABILITY WITH MULTICELL COORDINATION

In this section, we consider coordinated MIMO and study the effect of interference cancellation on coverage probability. We consider a user-centric multicell coordination whereby a user selects a cluster of BSs denoted as $\mathcal{B} = \{\mathrm{BS}_1, ..., \mathrm{BS}_K\}$ that are able to share CSIs of their respective users to cancel the interference experienced by him. Since our focus here is on the interference cancellation and its impact on coverage, we simply assume SU-MIMO and constant power allocation $\eta = 0$. However, the analysis can be straightforwardly extended to MU-MIMO and general fractional power control cases.

For the sake of tractability of analysis, a new parameter ρ is introduced to designate the coordination distance ratio, it is defined as ratio of the user distance to its serving BS BS_1 over its distance to the first interfering BS BS_K, i.e. $\rho = \frac{r_1}{r_K}$. This parameter defines the coordination range inside which the interference is to be eliminated using coordinated beamforming technique. Moreover, this parameter sheds light on where the coordination strategy is more beneficial than transmission with no coordination. Although the analysis can be conducted by averaging over all randomness involved in the assumed scenario, we will set out our analysis based on

the conditional coverage probability for a given value of ρ. The following theorem gives the conditional probability of coverage.

Theorem 3: The upper bound of coverage probability in cellular systems employing interference cancellation using coordinated-MIMO and conditioned on ρ with path-loss $\alpha = 4$, $P_c^{\mathsf{CB}}(\rho)$, is given as

$$P_c^{\mathsf{CB}}(\rho) \leq \frac{(\lambda\pi)}{(2G(\bar{\gamma},\rho)+1)^K} \sum_{m=1}^{\Delta} \binom{\Delta}{m}(-1)^{m+1} \sum_{n=0}^{K-1} \frac{(\lambda\pi)^n(2G(\bar{\gamma},\rho)+1)^n}{n!}\mathcal{G}_n(\bar{\gamma},\rho) \quad (20)$$

where:

$$\mathcal{G}_n(\bar{\gamma},\rho) = (2Z)^{-\frac{n+1}{2}}\Gamma(n+1)\exp\left(\frac{\big(\lambda\pi(G(\bar{\gamma},\rho)+1)\big)^2}{4Z}\right)D_{-(n+1)}\left(\sqrt{\frac{2}{Z}}\lambda\pi\big(G(\bar{\gamma},\rho)+1\big)\right)$$
$$(21)$$

$$G(\bar{\gamma},\rho) = \frac{m\kappa\bar{\gamma}\rho^\alpha}{\alpha-2}{}_2F_1\left(1,1-\frac{2}{\alpha};2-\frac{2}{\alpha};-m\kappa\bar{\gamma}\rho^\alpha\right) \quad (22)$$

$$Z = \frac{\sigma^2 m\kappa\bar{\gamma}}{P} \quad (23)$$

where $\kappa = (\Delta!)^{(-1/\Delta)}$ and $\Delta = N_t - K + 1$.
D_{-v} denote the parabolic cylinder function.

Proof: See Appendix D. ∎

V. EFFECTIVE CAPACITY ANALYSIS

In this section, analytical expression are introduced for effective capacity. The effective capacity can be expressed in terms of coverage probability, and thus it will be defined as a function of the key system parameters; BSs density, path-loss, power control policy, and antenna number. For multicell setting, the effective capacity quantifies the average of maximum arrival rate supportable by a system with inter-cell interference. It can also be interpreted as (i) the average of the maximum arrival rate that the system can support for a randomly chosen user, (ii) the average fraction of users for whom the maximum arrival rate can be supported, (ii) the average fraction of the network area for which the maximum arrival rate can be supported. The following theorem gives the effective capacity expression.

Theorem 4: For a given QoS exponent θ, the upper bound of effective capacity in multicell cellular systems can be approximated by:

$$E_c \approx -\frac{1}{\theta}\ln\left(1 - \sum_{n=1}^{N}\omega_n f(x_n)\right) \quad (24)$$

where x_n and ω_n are the nth zero of the Hermite polynomial $H_n(x_n)$ of degree N, and the corresponding weight of the function $f(.)$ at the nth abscissa respectively. The $f(x_n)$ is the coverage probability of the system with $\bar{\gamma} = m\kappa\big(x_n^{\frac{-1}{\theta}} - 1\big)$.

Proof: See Appendix E. ∎

VI. NUMERICAL RESULTS

This section provides the simulation and analytical results of coverage probability and effective capacity for both considered scenarios. To simulate PPP model, we first consider a bounded area of 10km^2. The density of BSs in this area is $\lambda = 1/(30000 * \pi^2)$ BS per m^2. The number of BSs follows Poisson distribution. Then, the BSs are distributed uniformly on the bounded area. The points distributed as such represents one realization of point process. We also consider a grid model assuming uniformly spaced square area of BSs. For simulation purposes, 36 BSs are positioned at regular distance from each other.

In Figs. 2(a) and (b), analytical expressions of coverage probability of SU-MIMO are compared with grid simulation for different antenna number for power control factors $\eta = 0, 1$, and assuming interference-limited case, i.e. $\sigma^2 = 0$. It can be clearly observed that the analytical expressions excellently approximate the simulation of coverage probability over the entire range of signal-to-interference ratio (SIR) of interest..

Similar observation can be made about Figs. 3(a) and (b) that show the comparison of simulation and analytical results of MU-MIMO system and coordinated MIMO, respectively, assuming $\sigma^2 = 0$. It can be clearly noticed that for both cases the analytical expressions approximate the analytical expressions for different antenna numbers and entire range of (SIR). Figs. 4(a) and (b) depict the coverage probability of SU-MIMO and MU-MIMO, respectively, as a function of power control strategies $\eta = 0, 0.25, 0.5, 1$, and antenna number $N_t = 2, 4$. It can be clearly observed the fact that for all η values, the coverage probability decreases with the increase of transmit antenna N_t in MU-MIMO (full SDMA) scheme, while increasing for SU-MIMO as shown clearly in Fig. 5, that compares between both schemes for different power control factors and $N_t = 2$. This is due to two reasons: firstly, ZF utilised in SDMA to cancel intra-user interference causes loss in degrees of freedom, hence degrading the signal quality. Secondly, more interference is generated with the increase in number of users served via SDMA. Despite the decrease in both coverage and average user rate with MU-MIMO scheme, the scheme serves more users and may results in higher sum rate in the system. This presents another delicate trade-off inherent in wireless systems between area spectral efficiency measured in (bits/sec/Hz/m^2) and user-link spectral efficiency given in (bits/sec/Hz). Noticeably, both SU-MIMO and MU-MIMO have an identical performance in terms of power control strategies;

the coverage probability of both is highest with fractional power control in low SIR threshold values, while the constant power allocation provides the best performance in higher SIR values. Now, let us focus our discussion on the impact of power control strategies on coverage probability in both SU-MIMO and MU-MIMO schemes. We consider the constant power $\eta = 0$ as the the reference of comparison. It can be clearly observed that for both SU-MIMO and MU-MIMO cases the constant power allocation almost gives comparable performance (coverage probability) to the cases ($\eta = 0.25, \eta = 0.5$) in low SIR thresholds, while outperforming all other power control strategies in high SIR values.

The largest coverage probability in the lower 50 percentile is provided by $\eta = 0.25$ followed by $\eta = 0.5$ before crossing below $\eta = 0$ case at $8.5\,\mathrm{dB}$ and $-4\,\mathrm{dB}$ for SU-MIMO and MU-MIMO (with $N_t = 2$), respectively. The difference in coverage for $\eta = 0, 0.25, 0.5$ is almost negligible in the low SIR thresholds. As η increases towards 1, the coverage decreases accordingly. The case η provides the lowest coverage across the entire range of SIR thresholds. The effect of power control can be fully explained by concentrating on the performance of cell-edge users relative to the cell-centre and the intrinsic trade-off between their performance. Cell-centre usually enjoy good channel conditions and are not susceptible to strong interference. Thus, they are typically noise-limited, and reducing the transmit power inevitably reduces their SIR. Considering this fact, constant power control is the optimal power strategy. On the other hand, cell-edge users typically more susceptible to high interference (interference-limited case). Hence, employing high power control factors such as $\eta = 1$ results in an increase in their SIR, while relatively reducing the transmit power of cell-centre users served by neighbouring BSs (interfering BSs). This disparity becomes more noticeable with high η values. Consequently, there is a delicate trade-off between increasing interference experienced by cell-edge users and reducing interference from cell-centre users at the neighbouring cells, giving rise to the fact that fractional values of η provides the highest coverage values for the majority of users.

Now let us assume that a typical BS serves only one user, i.e. SU-MIMO, but uses the rest of its degrees of freedom to cancel the interference on the users in neighbouring cells. Fig. 6 provides the coverage probability of coordinated MIMO as a function of ρ, and compares between no coordination with coordination schemes. As previously discussed, coordination causes loss in degrees of freedom and thereby lowering SIR. This loss of degrees of freedom may be disadvantageous when the nearer interferers are far away from the user, therefore, in this case,

no coordination, i.e. transmitting through MRT, is preferable as it exploits the whole degrees of freedom provided by the system. This case corresponds to the lower values of ρ as shown in Fig. 6. However, when the interferes get closer, i.e. $\rho = 0.95$, coordination becomes more useful to enhance the coverage for the system. When $\rho = 0.8$, for low SIR thresholds MRT performs better than CB before crossing below CB curve in -6 dB, where CB outperforms MRT.

Fig. 7 depicts the performance of E_c for SU-MIMO and MU-MIMO as a function of power control factor. Similar to the coverage probability, the performance of E_c for SU-MIMO scheme is noticeably better than that of MU-MIMO due to the same reason mentioned previously. Notice that when θ gets larger, E_c approaches 0, suggesting that the system is incapable of supporting the arrival rate when the delay constraint is very stringent.

For both schemes, it can also be clearly observed that for low delay constraints i.e. $\theta \to 0$, lower power control factors provide comparable performance with the strategy of $\eta = 0$ being the best over all. When delay constraint gets more stringent $\theta \to \infty$, fractional power control strategy outperforms the others, in particular $\eta = 0.25$ yields the best performance. Note that the strategy of $\eta = 1$ gives the worst performance over the entire range of θ values. When the delay constraint gets looser, i.e. small θ, it might be better to transmit with power control factors less than 0.25. While in case of stringent delay constraint, transmitting with power $\eta = 0.25$ provides the best performance. These observations suggest that fractional power control of $\eta \leq 0.25$ is the best strategy among all others for enhancing E_c in interference-limited scenarios.

The impact of power control factor on E_c can be understood by noticing the behaviour of E_c with respect to θ. When the delay constraints θ becomes more stringent, the best power policy is to compensate for the path-loss and keep the rate as fixed as possible calling for using power control factor $0.5 > \eta > 0$. Although a strategy with large values of θ keeps a user with fixed SIR (hence fixed rate), it cause strong interference to the cell-edge of neighbouring cells or deprive cell-centre users from high SIR gain that is necessary for QoS guarantee.

VII. CONCLUSIONS

This paper studied coverage probability and effective capacity in MIMO downlink cellular networks employing distance-based power control. The BSs are assumed to be distributed according spatial PPP model. Tractable, analytical expressions for coverage probability and effective capacity are derived for two system scenarios; in the first scenario, fractional power control is

employed with no multicell coordination, while in the second, the system is assumed to employ coordination. For the first scheme, closed-form expressions for Laplace transform accounting for interference are introduced for special cases. Then, novel, tractable expression for effective capacity are derived in terms of coverage probability. These expressions are functions of the main system parameters which can give an insight on the system design guide. The numerical results shows that for coverage probability, the strategy of power control factor $\eta \leq 0.25$ is the best in low thresholds, while constant power allocation outperforms the others in high thresholds. Moreover, for effective capacity the constant power allocation strategy performs better in low QoS constraints, while fractional power control factors, i.e. $\eta \leq 0.25$, outperforms the other strategies in high QoS constraints. For the second scheme, the same analysis is carried out to derive analytic expressions for coverage probability and effective capacity as functions of coordination distance ratio ρ. Numerical results reveal that coordination performs better when the interferers are close enough to the served user, while MRT is better when the interferers are far enough from the served user.

APPENDIX A
PROOF OF THEREOM 1

Since $g_0 \sim \Gamma(N_t, 1)$, and its CCDF is the regularized gamma function given by $\frac{\gamma(N_t, x)}{\Gamma(N_t)} = \int_0^x \frac{t^{N_t-1}e^{-t}}{\Gamma(N_t)}\mathrm{d}t$, we use the bounds on the CCDF given as [28]

$$(1 - e^{-\zeta x})^{N_t} \leq \frac{\gamma(N_t, x)}{\Gamma(N_t)} \leq (1 - e^{-x})^{N_t} \tag{25}$$

using binomial expansion yields

$$\sum_{m=1}^{N_t} \binom{N_t}{m}(-1)^{m+1}e^{-\zeta mx} \geq \frac{\gamma(N_t, x)}{\Gamma(N_t)} \geq \sum_{m=1}^{N_t} \binom{N_t}{m}(-1)^{m+1}e^{-mx} \tag{26}$$

then we have:

$$\begin{aligned}
P_c^{\mathsf{SU}} &= \int_{r_1 \geq 0}^{\infty} \mathbb{P}\left[\frac{g_0 r_1^{\alpha(\eta-1)}}{(\sigma^2 + I)} \geq \bar{\gamma}|r_1\right] f_{r_1}(r_1)\mathrm{d}r_1 \\
&= \int_{r_1 \geq 0}^{\infty} \mathbb{P}\left[g_0 \geq r_1^{\alpha(1-\eta)}\bar{\gamma}(\sigma^2 + I)|r_1\right] f_{r_1}(r_1)\mathrm{d}r_1 \\
&\overset{a}{\leq} \int_{r_1 \geq 0}^{\infty} \sum_{m=1}^{N_t} \binom{N_t}{m}(-1)^{m+1}e^{-\bar{\gamma}m\zeta r_1^{\alpha(1-\eta)}\sigma^2}\mathbb{E}\{e^{-sI}|r_1\} f_{r_1}(r_1)\mathrm{d}r_1
\end{aligned} \tag{27}$$

where $s = \bar{\gamma}m\zeta r_1^{\alpha(1-\eta)}$, the inequality in (a) stems from substituting the upper bound of $\frac{\gamma(N_t,x)}{\Gamma(N_t)}$ in (26). The Laplace term, i.e., $\mathbb{E}\{e^{-sI} \mid r_1\}$ that is conditioned on r_1, can be obtained as follows [19]:

$$
\begin{aligned}
\mathbb{E}\{e^{-sI} \mid r_1\} &= \mathbb{E}_{\Phi,g_i,X_i}\left\{e^{-s\sum_{i\in\Phi/\{BS_1\}} g_i X_i^{\alpha\eta} r_i^{-\alpha}}\right\} \\
&= \mathbb{E}_{\Phi,X_i,\{g_i\}}\left\{\left(\prod_{i\in\Phi/\{b_1\}} e^{-sg_i X_i^{\alpha\eta} r_i^{-\alpha}}\right)\right\} \\
&= \mathbb{E}_\Phi\left\{\left(\prod_{i\in\Phi/\{b_1\}} \mathbb{E}_{g_i,X_i}\left\{e^{-sg_i X_i^{\alpha\eta} r_i^{-\alpha}}\right\}\right)\right\} \\
&\overset{a}{=} \exp\left(-2\pi\lambda \int_{r_1}^\infty \left(1 - \mathbb{E}_{g,X}\left\{e^{-sgX^{\alpha\eta}v^{-\alpha}}\right\}\right)v\,dv\right) \\
&\overset{b}{=} \exp\left(-2\pi\lambda\mathbb{E}_X\left\{\int_{r_1}^\infty \frac{(1+sX^{\alpha\eta}v^{-\alpha})^\Psi - 1}{(1+sX^{\alpha\eta}v^{-\alpha})^\Psi}v\,dv\right\}\right) \\
&\overset{c}{=} \exp\left(-2\pi\lambda\mathbb{E}_X\left\{\int_{r_1}^\infty \frac{\sum_{m=1}^\Psi \binom{\Psi}{m}(sX^{\alpha\eta}v^{-\alpha})^m}{(1+sX^{\alpha\eta}v^{-\alpha})^\Psi}v\,dv\right\}\right)
\end{aligned}
$$

where (a) follows from the probability generating functional (PGFL) property of a PPP [19]. (b) stems from the independence between Φ and both channel fading g and X, and evaluating the expectation over g, i.e. $\Gamma(\Psi,1)$. (c) yields from binomial expansion. For SU-MIMO, we have $\Psi = 1$, by substituting in Ψ, and evaluating the inner integration as

$$
\int_{r_1}^\infty \frac{v}{1 + s^{-1}X^{-\alpha\eta}v^\alpha}dv = sX^{\alpha\eta}\frac{r_1^{\frac{2-\alpha}{\alpha}}}{\alpha-2}{}_2F_1\left(1, 1 - \frac{2}{\alpha}; 2 - \frac{2}{\alpha}; -\frac{sX^{\alpha\eta}}{r_1^\alpha}\right) \tag{28}
$$

we have

$$
\mathbb{E}\{e^{-sI} \mid r_1\} = \exp(-2\pi\lambda\psi) \tag{29}
$$

where ψ is given by (13). By plugging (1) (for $K = 1$) and (29) in (27), (12) follows immediately.

APPENDIX B
PROOF OF COROLLARY 1

Assuming that the distance between each interfering BS and its served user referred to as X is a r.v. following Rayleigh distribution as proven by [26], for given values of $\alpha = 4$ and $\eta = 0$, expressing the hypergeometric function as an infinite series, invoking the relation $\Gamma(a,b) =$

$(a)_b\Gamma(a)$, and implementing integration and some algebraic manipulations [29], we have the following

$$
\begin{aligned}
\psi &= \mathbb{E}_X\left\{\frac{\bar{\gamma}r_1^{(2-\alpha\eta)}X^{\alpha\eta}}{\alpha-2}{}_2F_1\left(1, 1-\frac{2}{\alpha}; 2-\frac{2}{\alpha}; -\bar{\gamma}r_1^{-\alpha\eta}X^{\alpha\eta}\right)\right\} \\[4pt]
&\overset{a}{=} \frac{\bar{\gamma}r_1^{(2-\alpha\eta)}}{\alpha-2}\int_0^\infty X^{\alpha\eta}{}_2F_1\left(1, 1-\frac{2}{\alpha}; 2-\frac{2}{\alpha}; -\bar{\gamma}r_1^{-\alpha\eta}X^{\alpha\eta}\right)(2\pi\lambda X e^{-\pi\lambda X^2})\mathrm{d}X \\[4pt]
&\overset{b}{=} \frac{2\pi\lambda\bar{\gamma}r_1^{(2-\alpha\eta)}}{\alpha-2}\int_0^\infty X^{\alpha\eta+1}e^{-\pi\lambda X^2}\sum_{n=0}^\infty \frac{(1)_n(1-2/\alpha)_n}{(2-2/\alpha)_n n!}(-\bar{\gamma}r_1^{-\alpha\eta}X^{\alpha\eta})^n \mathrm{d}X \\[4pt]
&\overset{c}{=} \frac{2\pi\lambda\bar{\gamma}r_1^{(2-\alpha\eta)}}{\alpha-2}\sum_{n=0}^\infty \frac{(1)_n(1-2/\alpha)_n(-\bar{\gamma}r_1^{-\alpha\eta})^n}{(2-2/\alpha)_n n!}\int_0^\infty X^{1+(1+n)\alpha\eta}e^{-\pi\lambda X^2}\mathrm{d}X \\[4pt]
&\overset{d}{=} \frac{2\pi\lambda\bar{\gamma}r_1^{(2-\alpha\eta)}}{\alpha-2}\sum_{n=0}^\infty \frac{(1)_n(1-2/\alpha)_n(-\bar{\gamma}r_1^{-\alpha\eta})^n}{(2-2/\alpha)_n n!}\frac{\Gamma\left(\frac{2+(1+n)\alpha\eta}{2}\right)}{2(\pi\lambda)^{(1+\frac{(1+n)\alpha\eta}{2})}} \\[4pt]
&\overset{e}{=} \frac{2\pi\lambda\bar{\gamma}r_1^{(2-\alpha\eta)}}{\alpha-2}\sum_{n=0}^\infty \frac{(1)_n(1-2/\alpha)_n(-\bar{\gamma}r_1^{-\alpha\eta})^n}{(2-2/\alpha)_n n!}\frac{\left(\frac{2+\alpha\eta}{2}\right)_{n\alpha\eta/2}\Gamma\left(\frac{2+\alpha\eta}{2}\right)}{2(\pi\lambda)^{(1+\frac{(1+n)\alpha\eta}{2})}} \\[4pt]
&\overset{f}{=} \frac{2\pi\lambda\bar{\gamma}r_1^{(2-\alpha\eta)}}{\alpha-2}\sum_{n=0}^\infty \frac{(-\bar{\gamma}r_1^{-\alpha\eta})^n(1)_n(1/2)_n}{2\pi\lambda(3/2)_n n!} \\[4pt]
&\overset{g}{=} \frac{\bar{\gamma}r_1^{(2-\alpha\eta)}}{\alpha-2}{}_2F_1(1, 1/2; 3/2; -\bar{\gamma}r_1^{-\alpha\eta})
\end{aligned}
\tag{30}
$$

where (a) comes from the assumption that the distance between each interfering BS and its served user referred to as X is a r.v. following Rayleigh distribution. In (b), the hypergeometric function is expressed as an infinite series by invoking the relation $\Gamma(a,b) = (a)_b\Gamma(a)$. In (c) and (d), we insert the integration inside the summation and integrating with respect to X, respectively. In (e), (f), and (g), we got an expression which can be expressed once again as a new hypergoemtric function by using the definition in (14) and simple mathematical simplifications.

APPENDIX C
PROOF OF THEOREM 2

Following similar steps of Appendix A and noticing that in full-SDMA $\Delta = 1$ and $\Psi = N_t$; the desired signal link is exponentially distributed, i.e. $g_0 \sim \exp(\mu)$, and $\mu = 1$, then we have

$$
\begin{aligned}
P_c^{\mathsf{MU}} &= \int_{r_1 \geq 0}^{\infty} \mathbb{P}\left[\frac{g_0 r_1^{\alpha(\eta-1)}}{(\sigma^2 + I)} \geq \bar{\gamma}|r_1\right] f_{r_1}(r_1) \mathrm{d}r_1 \\
&= \int_{r_1 \geq 0}^{\infty} \mathbb{P}\left[g_0 \geq r_1^{\alpha(1-\eta)}\bar{\gamma}(\sigma^2 + I)|r_1\right] f_{r_1}(r_1) \mathrm{d}r_1 \\
&= \int_{r_1 \geq 0}^{\infty} \mathbb{E}_I\left\{\exp(-\bar{\gamma} r_1^{\alpha(1-\eta)}(\sigma^2 + I)) \mid r_1\right\} f_{r_1}(r_1) \mathrm{d}r_1 \\
&= \int_{r_1 \geq 0}^{\infty} e^{-\bar{\gamma} r_1^{\alpha(1-\eta)}\sigma^2} \mathbb{E}_I\left\{e^{-\bar{\gamma} r_1^{\alpha(1-\eta)}} \mid r_1\right\} f_{r_1}(r_1) \mathrm{d}r_1
\end{aligned}
\tag{31}
$$

To evaluate $\mathbb{E}_I\left\{e^{-\bar{\gamma} r_1^{\alpha(1-\eta)}} \mid r_1\right\}$, let $s = \bar{\gamma} r_1^{\alpha(1-\eta)}$, by following the same approach in Appendix A for evaluating Laplace transform, we have

$$
\mathbb{E}\{e^{-sI} \mid r_1\} = \exp(-2\pi\lambda\psi)
\tag{32}
$$

where ψ is given by(19). By plugging (32) in (31), (18) follows immediately.

APPENDIX D
PROOF OF THEOREM 3

Similarly, by considering the upper bound of coverage probability as in the Appendix A, we have:

$$
\begin{aligned}
P_c^{\mathsf{CB}} &= \mathbb{E}_{r_1, r_K}\left\{\mathbb{P}\left[g \geq \frac{r_1^{\alpha}\bar{\gamma}}{P}(\sigma^2 + I_c)|r_1, r_K\right]\right\} \\
&\leq \mathbb{E}_{r_1, r_K}\left\{\sum_{m=1}^{\Delta}\binom{\Delta}{m}(-1)^{m+1} e^{-Zr_1^{\alpha}} \mathbb{E}_{I_c}\left\{e^{-\frac{m\kappa\bar{\gamma}}{P}r_1^{\alpha}I_c}|r_1, r_K\right\}\right\}
\end{aligned}
\tag{33}
$$

where $\Delta = N_t - K + 1$, and Z given by (23), and I_c is the the aggregate interference coming from all BSs in the point process Φ_c, defined as $\Phi_c = \Phi/\{\mathrm{BS}_1, ..., \mathrm{BS}_K\}$.

Note that since the nearest interferer is located at distance r_K, we condition the Laplace transform in (33) on both r_1 and r_K. Similarly, the Laplace transform can be obtained following the same approach, by denoting $s = \frac{m\kappa\bar{\gamma}}{P}r_1^{\alpha}$, and substituting for ρ as $\rho = \frac{r_1}{r_K}$, then we have

$$
\mathbb{E}_{I_c}\{e^{-sI_c}\} = \exp\left(-2\pi\lambda f(\bar{\gamma}, \alpha)\right)
\tag{34}
$$

where $f(\bar{\gamma}, \alpha) = r_K^2 G(\bar{\gamma}, \rho)$, and $G(\bar{\gamma}, \rho)$ is given by (22).

Plugging (34) in (33) and de-conditioning on both r_1 and r_K yields the following:

$$P_c^{\mathsf{CB}} \leq \int_0^\infty f_{r_1}(r_1) \int_{r_1}^\infty f_{r_K}(r_K) \overbrace{\sum_{m=1}^\Delta \binom{\Delta}{m}(-1)^{m+1} e^{-Zr_1^\alpha} \mathbb{E}_\rho\left\{ e^{-2\pi\lambda G(\bar{\gamma},\rho)r_K^2} \big| \rho \right\}}^{\mathcal{I}_2} \mathrm{d}r_K \mathrm{d}r_1$$

$$\leq \mathbb{E}_\rho\left\{ \int_0^\infty f_{r_1}(r_1) \underbrace{\int_{r_1}^\infty f_{r_K}(r_K) \sum_{m=1}^\Delta \binom{\Delta}{m}(-1)^{m+1} e^{-Zr_1^\alpha} e^{-2\pi\lambda G(\bar{\gamma},\rho)r_K^2} \mathrm{d}r_K}_{\mathcal{I}_1} \mathrm{d}r_1 \big| \rho \right\} \quad (35)$$

Since r_1, r_K, and ρ variables are independent of each other, we interchange the integration order using Fubini's theorem. Accordingly, after substituting (1) in (35), we have

$$\mathcal{I}_1 = \sum_{m=1}^\Delta \binom{\Delta}{m}(-1)^{m+1} e^{-Zr_1^\alpha} \int_{r_1}^\infty f_{r_K}(r_K) e^{-2\pi\lambda G(\bar{\gamma},\rho)r_K^2} \mathrm{d}r_K$$

$$= \sum_{m=1}^\Delta \binom{\Delta}{m}(-1)^{m+1} e^{-Zr_1^\alpha} \int_{r_1}^\infty e^{-\lambda\pi r_K^2} e^{-2\pi\lambda r_K^2 G(\bar{\gamma},\rho)} \left(\frac{2(\lambda\pi)^K r_K^{(2K-1)}}{\Gamma(K)} \right) \mathrm{d}r_K$$

$$= \frac{2(\pi\lambda)^K}{\Gamma(K)} \sum_{m=1}^\Delta \binom{\Delta}{m}(-1)^{m+1} e^{-Zr_1^\alpha} \frac{\Gamma\left(K, \lambda\pi(2G(\bar{\gamma}, \rho) + 1)r_1^2 \right)}{2\left(2\lambda\pi G(\bar{\gamma}, \rho) + \lambda\pi \right)^K} \quad (36)$$

where the last result can be obtained by utilising the integral identity: $\int_u^\infty x^m e^{-\beta x^n} \mathrm{d}x = \frac{\Gamma(v, \beta u^n)}{n\beta^v}$.

Plugging (36) and (1) with $K = 1$ in (35) and considering $\mathcal{I}_2$, we have:

$$\mathcal{I}_2 = \frac{2(\pi\lambda)^K}{\Gamma(K)} \sum_{m=1}^\Delta \binom{\Delta}{m} \frac{(-1)^{m+1}}{2\left(2\lambda\pi G(\bar{\gamma}, \rho) + \lambda\pi \right)^K} \int_0^\infty \Gamma\left(K, \lambda\pi(2G(\bar{\gamma}, \rho) + 1)r_1^2 \right) e^{-\lambda\pi r_1^2}$$

$$\times e^{-Zr_1^\alpha}(2\lambda\pi r_1)\mathrm{d}r_1 \quad (37)$$

By expressing the gamma function in (37) as $\Gamma(s, x) = (s-1)! e^{-x} \sum_{n=0}^{s-1} \frac{x^n}{n!}$, doing some mathematical manipulations, and conditioning on ρ, we have:

$$P_c^{\mathsf{CB}}(\rho) \leq \frac{\pi\lambda}{2\left(2G(\bar{\gamma}, \rho) + 1 \right)^K} \sum_{m=1}^\Delta \binom{\Delta}{m}(-1)^{m+1} \sum_{n=0}^{K-1}$$

$$\times \int_0^\infty e^{-\left(\lambda\pi\left(2G(\bar{\gamma},\rho)+1 \right)+\lambda\pi \right)r_1^2} e^{-Zr_1^\alpha} \frac{\left(\lambda\pi\left(2G(\bar{\gamma}, \rho) + 1)r_1^2 \right) \right)^n}{n!}(2\lambda\pi r_1)\mathrm{d}r_1 \quad (38)$$

Notice that the above expression is the conditional probability of coverage represented as a function of ρ, so we omit the expectation symbol. This integral can be evaluated numerically, and it can be obtained in a closed-form for a special case of $\alpha = 4$, and is given by:

$$P_c^{\mathsf{CB}}(\rho) \leq \frac{\pi\lambda}{2\Big(2G(\bar{\gamma},\rho)+1\Big)^K} \sum_{m=1}^{\Delta} \binom{\Delta}{m}(-1)^{m+1} \sum_{n=0}^{K-1} \frac{(\lambda\pi)^n}{n!}\Big(2G(\bar{\gamma},\rho)+1\Big)^n \mathcal{G}_n(\bar{\gamma},\rho) \quad (39)$$

where $\mathcal{G}_n(\bar{\gamma},\rho)$ and $G(\bar{\gamma},\rho)$ are given in (21) and (22), respectively. The above result, can be obtained by changing the variable $r_1^2 = x$ and invoking the integral identity $\int_0^\infty x^{v-1}e^{-\beta x^2-\gamma x}\mathrm{d}x = (2\beta)^{-v/2}\Gamma(v)\exp(\frac{\gamma^2}{8\beta})D_{-v}(\frac{\gamma}{\sqrt{2\beta}})$.

APPENDIX E
PROOF OF THEOREM 4

Starting from (12), and using the following identity: $\mathbb{E}\{x\} = \int_{t\geq0}^\infty \mathbb{P}[x \geq t]\mathrm{d}t$, where the expectation operation is defined over all randomness involved in the SINR, we have the following:

$$\mathbb{E}\Big\{1+SINR\Big\}^{-\theta} = \int_{r_1\geq0}^\infty \int_{t\geq0}^1 f_{r_1}(r_1)\mathbb{P}\Big[\Big(1+SINR\Big)^{-\theta} > t|r_1\Big]\mathrm{d}t\mathrm{d}r_1 \quad (40)$$

$$= \int_{r_1\geq0}^\infty \int_{t\geq0}^1 f_{r_1}(r_1)\mathbb{P}\Big[SINR < (t^{\frac{-1}{\theta}}-1)|r_1\Big]\mathrm{d}t\mathrm{d}r_1 \quad (41)$$

$$= 1 - \int_{r_1\geq0}^\infty \int_{t\geq0}^1 f_{r_1}(r_1)\mathbb{P}\Big[SINR \geqslant t^{\frac{-1}{\theta}}-1|r_1\Big]\mathrm{d}t\mathrm{d}r_1 \quad (42)$$

by substituting for the upper bound of coverage probability in the above integration and approximating the integration in (42) by Gauss-Hermite quadrature given by [27]:

$$\int_0^1 x^k f(x)\mathrm{d}x \approx \sum_{n=1}^N \omega_n f(x_n) \quad (43)$$

(24) follows immediately.

REFERENCES

[1] Cisco Visual Networking Index: Global Mobile Data Traffic Forecast Update, 2010-2015. White Paper, Feb. 2011.

[2] 3GPP LTE Release 10 & Beyond (LTE-Advanced), 3rd Generation Partnership Project (3GPP), 2009. [Online]. Available:http://www.3gpp.org/

[3] R. Baldemair, E. Dahlman, G. Fodor, G. Mildh, S. Parkvall, Y. Seln, H. Tullberg, and K. Balachandran, "Evolving wireless communications: addressing the challenges and expectations of the future," *IEEE Trans. Veh. Mag.*, vol. 8, no. 1, pp. 24-30, Mar. 2013.

[4] J. G. Andrews, S. Buzzi, W. Choi, S. V. Hanly, A. Lozano, A. C. K. Soong, and J. Charlie, "What will 5G be?," *IEEE J. Sel. Areas Commun.*, vol. 32, no. 6, pp. 1065C1082, Jun. 2014.

[5] A. Gupta and R. Kumar Jha, " A survey of 5G networks: architecture and emerging technologies," *IEEE Access.*, vol. 2, pp. 1187C1195, Jul. 2014.

[6] T. M. Cover and J. A. Thomas, *Elements of Information Theory*, New York: Wiley, 1991.

[7] X. Zhang and J. Tang, "Power-delay tradeoff over wireless networks," *IEEE Trans.Commun.*, vol. 61, no. 9, pp. 3673-3684, Sept. 2013.

[8] Y. Cui, V. K. N. Lau, R. Wang, H. Huang, S. Zhang, "A survey on delay-aware resource control for wireless systems-large deviation theory, stochastic Lyapunov drift, and distributed stochastic learning," *IEEE Trans. Inf. Theory*, vol. 58, no. 3, pp. 1677-1701, Mar. 2012.

[9] X. Lin, N. B. Shroff, and R. Srikant, "A tutorial on cross-layer optimization in wireless networks," *IEEE J. Sel. Areas Commun.*, vol. 24, no. 8, pp. 1452-1463, Aug. 2006.

[10] D. Wu and R. Negi, "Effective capacity: A wireless link model for support of quality of service," *IEEE Trans. Wireless Commun.*, vol. 2, no. 4, pp. 630-643, July 2003.

[11] C.-S. Chang, "Effective bandwidth in high-speed digital networks," *IEEE J. Sel. Areas Commun.*, vol. 13, no. 6, pp. 1091-1100, Aug. 1995.

[12] C.-S. Chang, "Stability, queue length, and delay of deterministic and stochastic queueing networks," *IEEE Trans. Automat. Control.*, vol. 39, no. 5, pp. 913-931, May 1994.

[13] L. Musavian and S. Aissa, "Effective capacity of delay-constrained cognitive radio in Nakagami fading channels," *IEEE Trans. Wireless Commun.*, vol. 9, no. 3, pp. 1054-1062, Mar. 2010.

[14] L. Musavian and S. Aissa, and S. Lambotharan, "Effective capacity for interference and delay constrained cognitive radio relay channels," *IEEE Trans. Wireless Commun.*, vol. 9, no. 5, pp. 1698-1707, May. 2010.

[15] J. Tang and X. Zhang, "Quality-of-Service driven power and rate adaptation for multichannel communications over wireless links," *IEEE Trans. Wireless Commun.*, vol. 6, no. 12, pp. 4349-4360, Dec. 2007.

[16] J. Tang and X. Zhang, "Cross-layer resource allocation over wireless relay networks for quality of service provisioning," *IEEE J. Sel. Areas Commun.*, vol. 25, no. 4, pp. 2318-2328, May 2007.

[17] J. Tang and X. Zhang, "Cross-layer-model based adaptive resource allocation for statistical qos guarantees in mobile wireless networks," *IEEE Trans. Wireless Commun.*, vol. 7, no. 6, pp. 2318-2328, Jun. 2008.

[18] M. Haenggi, J. Andrews, F. Baccelli, O. Dousse, and M. Franceschetti, "Stochastic geometry and random graphs for the analysis and design of wireless networks," *IEEE J. Sel. Areas in Commun.*, vol. 27, no. 7, pp. 1029C1046, Sept. 2009.

[19] J. Andrews, F. Baccelli, and R. Ganti, "A tractable approach to coverage and rate in cellular networks," *IEEE Trans. Commun.*, vol. 59, no. 11, pp. 3122-3134, Nov. 2011.

[20] N. Jindal, S. Weber, and J. Andrews, "Fractional power control for decentralized wireless networks," *IEEE Trans. Wireless Commun.*, vol. 7, no. 12, pp. 5482-5492, Dec. 2008.

[21] H. Haas, S. McLaughli, *Next Generation Mobile Access Technologies: Implementing TDD*, Cambridge University Press, 2007.

[22] B. Rong, C.-H. Liu and S. Cui, "Discrete location-dependent power control in wireless clustered ad hoc networks," in *Proc. IEEE GLOBECOM '13*, Dec. 2013.

[23] T. Novlan, H. Dhillon, and J. Andrews, "Analytical modelling of uplink cellular networks," *IEEE Trans. Wireless Commun.*, vol. 12, no. 6, pp. 2669-2679, June 2013.

[24] J. Zhang, J. Andrews, "Adaptive spatial intercell interference cancellation in multicell wirless networks," *IEEE J. Sel. Areas in Commun.*, vol. 28, no. 8, pp. 1455-1468, Dec. 2010.

[25] H. Dhillon, M. Kountouris and J. Andrews, "Downlink MIMO HetNets: modeling, ordering results and performance analysis ," *IEEE Trans. Wireless Commun.*, vol. 12, no. 10, pp. 5208-5222, Oct. 2013.

[26] M. Haenggi, "On distances in uniformly random networks," *IEEE Trans. Inf. Theory.*, vol. 51, no. 10, pp. 3584-3586, Oct. 2005.

[27] M. Abramowitz and I. A. Stegun, *Handbook of Mathematical Functions with Formulas, Graphs, and Mathematical Tables*, 9th edition. Dover, 1965.

[28] K. Huang, R. W. Heath, and J.G. Andrews, "Space division multiple access With a sum feedback rate constraint," *IEEE Trans. Signal Process.*, vol. 55, no.7, pp.3879-3891, July 2007.

[29] I. S. Gradshteyn and I. M. Ryzhik, *Table of Integrals, Series, and Products*, 7th edition. Academic Press, 2007.
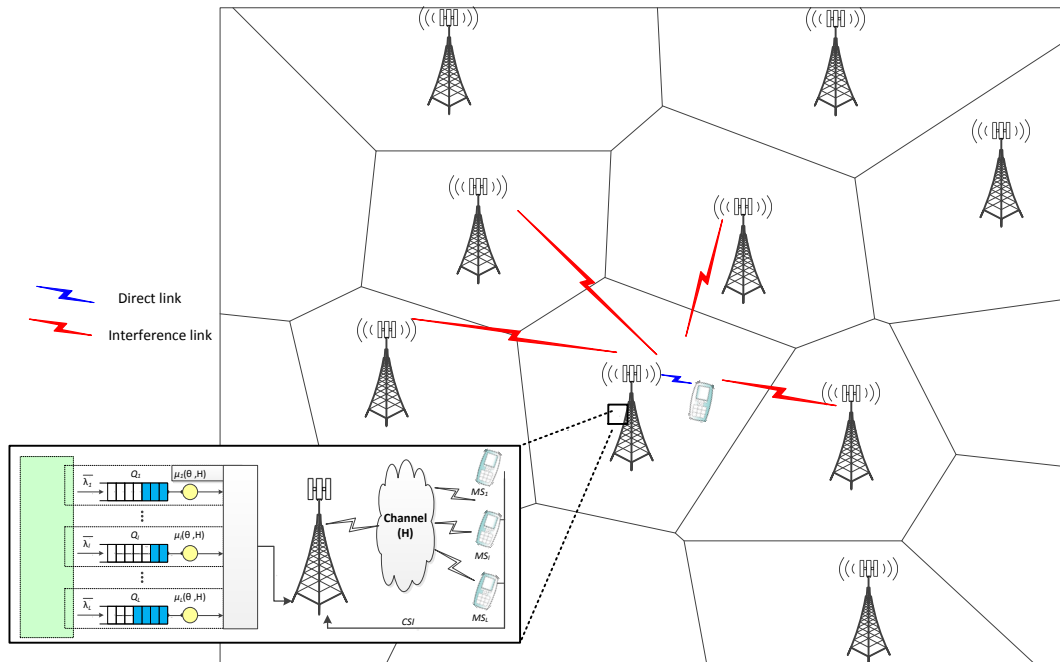
Fig. 1.   An illustration of random network configuration, BSs are distributed randomly in two-dimensional space, and each BS has queues for packet accumulation. The scheduler serves a user (or multiple users in MU-MIMO) according the rule scheduling that should incorporates θ of the user.
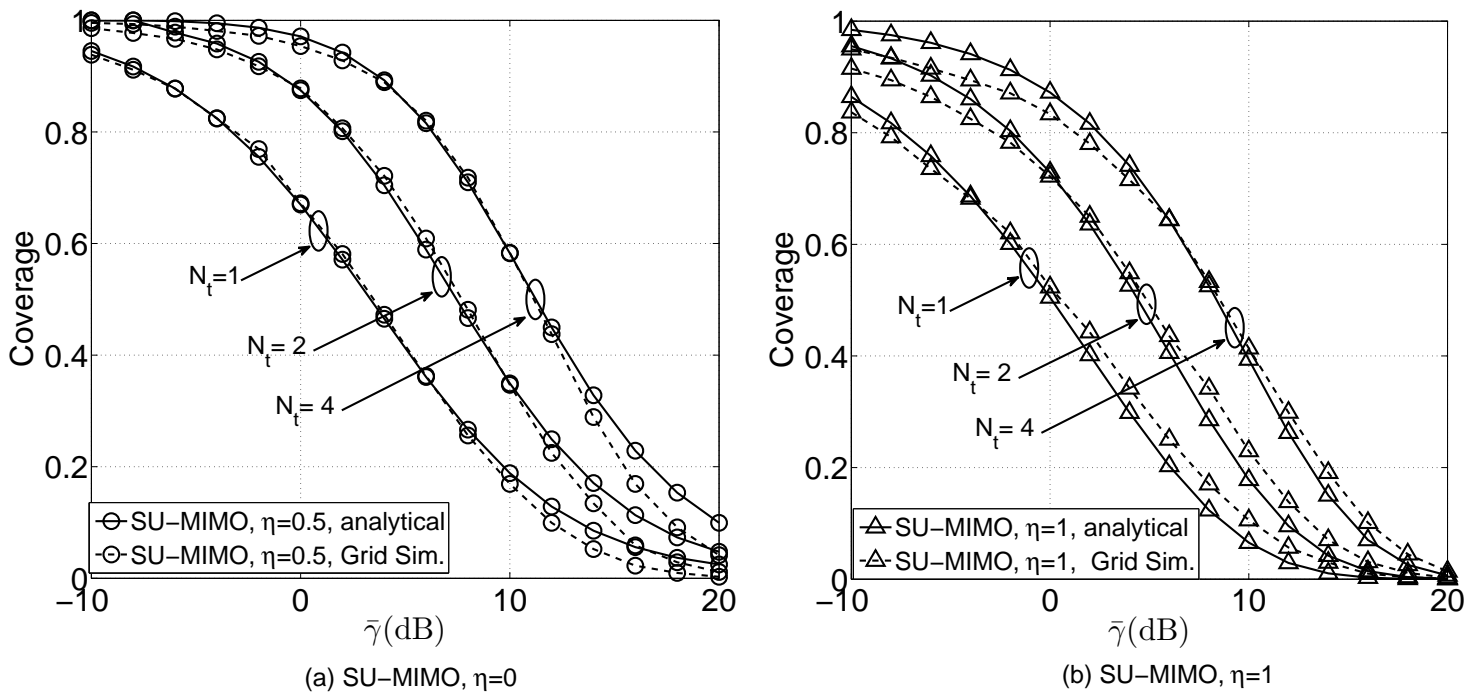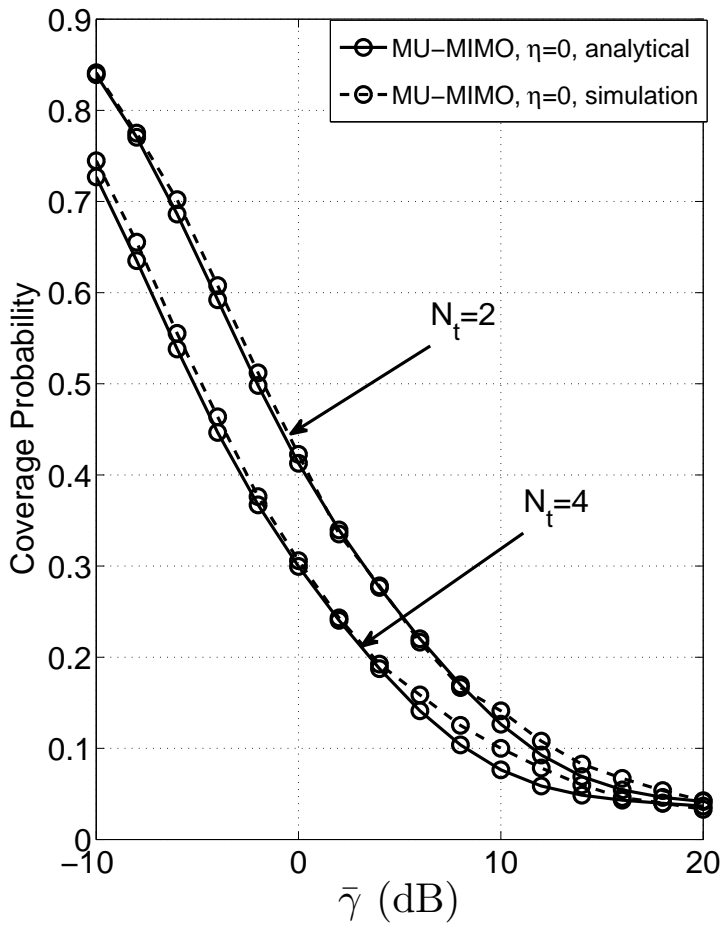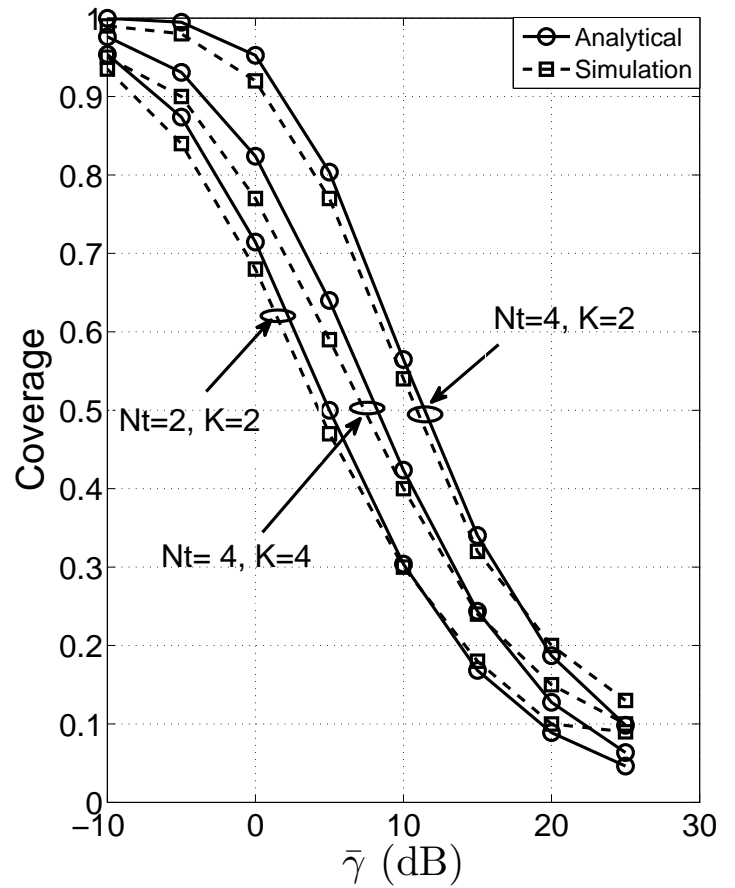
Fig. 2. Simulation results of coverage probability of SU-MIMO, ($N_t = \{1, 2, 4\}$, $\eta = \{0, 1\}$, $\sigma^2 = 0$).

(a) MU–MIMO

(b) Coordinated–MIMO

Fig. 3. (a) shows the comparison with simulation results for MU-MIMO, ($N_t = \{2, 4\}$, $\eta = 0$, $\sigma^2 = 0$). (b) shows the comparison with simulation results for coordinated-MIMO, ($\eta = 0$, $N_t = \{2, 4\}$, $K = \{2, 4\}$, $\sigma^2 = 0$).
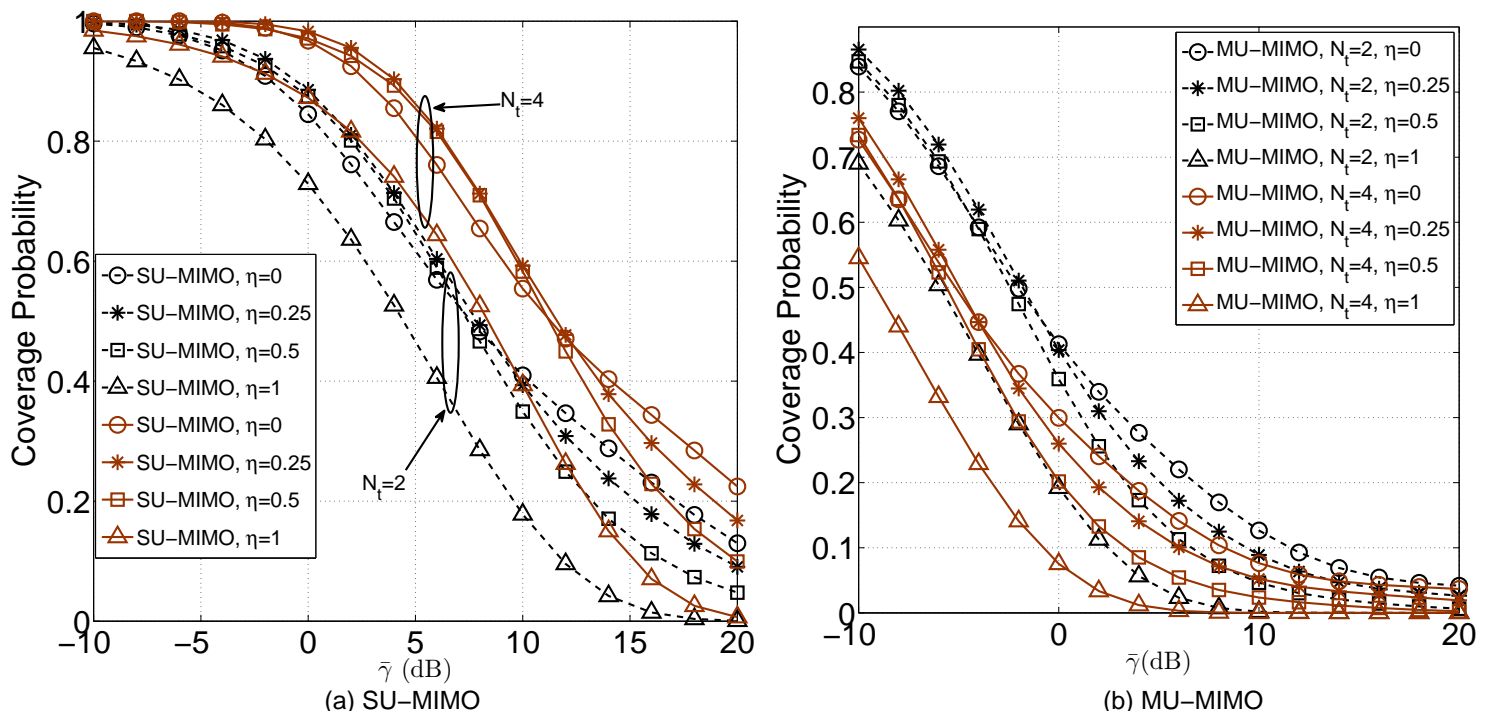
Fig. 4. (a) and (b) show the the coverage probability for SU-MIMO and MU-MIMO, respectively for various fractional power control strategies are shown in both cases. ($\eta = 0, 0.25, 0.5, 1$, $N_t = \{2, 4\}$, $\sigma^2 = 0$).
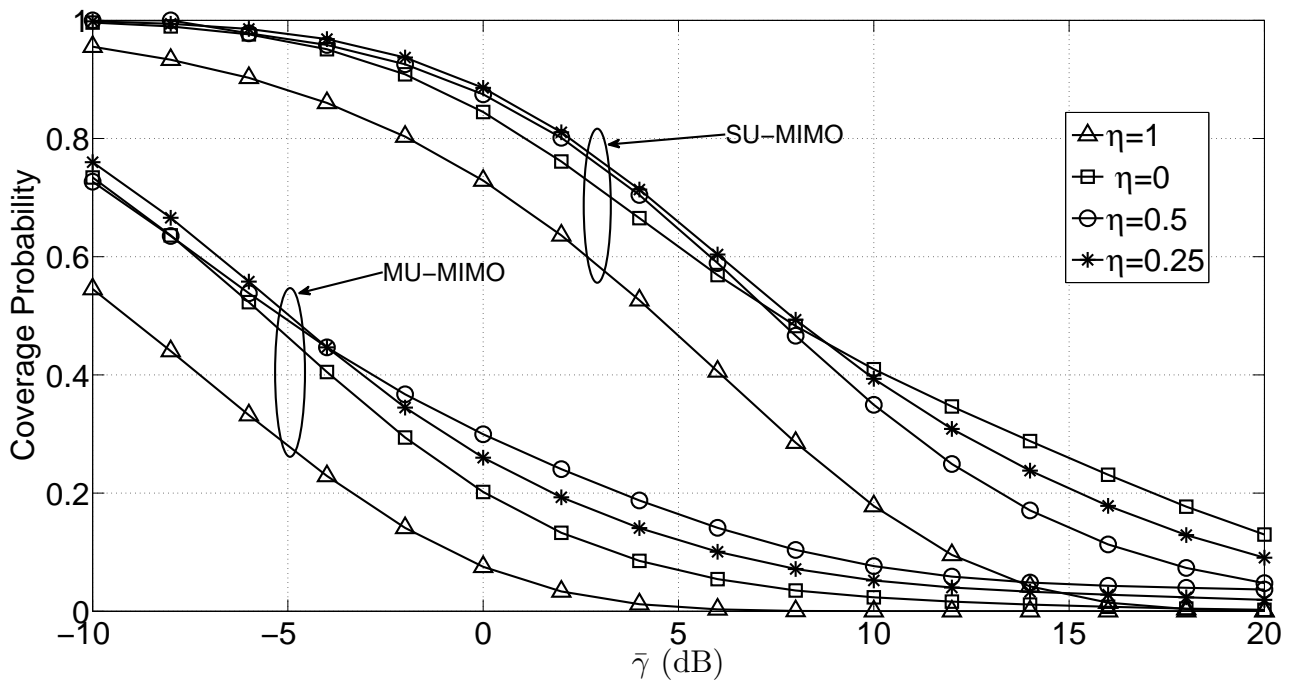
Fig. 5. Comparison between SU-MIMO and MU-MIMO for different power control strategies; ($\eta = 0, 0.5, 1$, $N_t = \{2, 4\}$, $\sigma^2 = 0$).
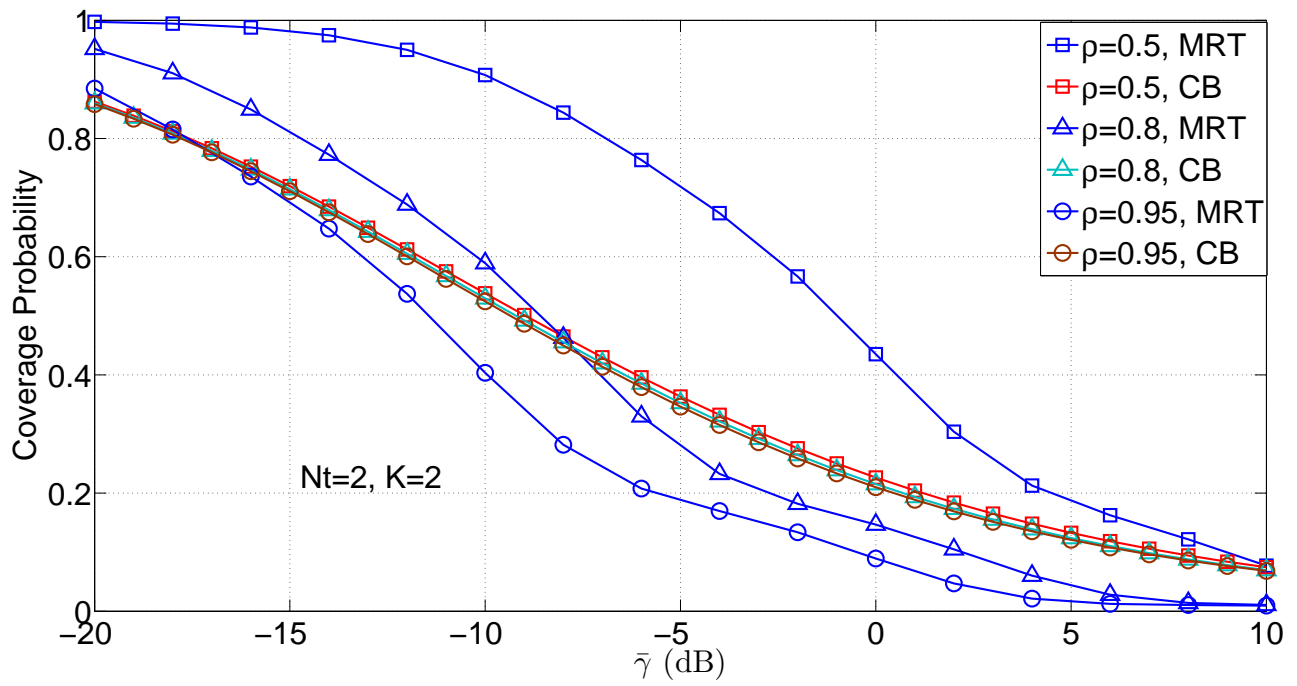
Fig. 6. Comparison between coordination using CB and no coordination using MRT for different ρ values, ($N_t = 2$, $P = 1$, $\sigma^2 = 0$).
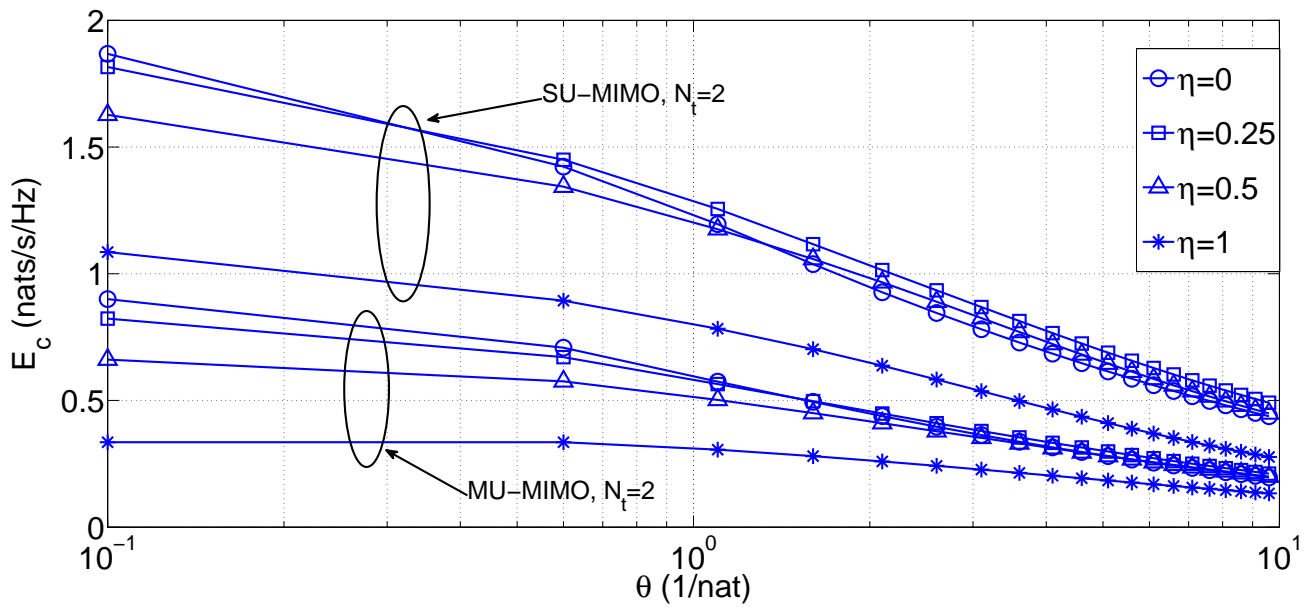
Fig. 7. Comparison of effective capacity of both SU-MIMO and MU-MIMO systems for different power control strategies; ($\eta = 0, 0.25, 0.5, 1, \sigma^2 = 0$).